

A Study of the Primary Breakup Process and Macroscale Characteristics of Impinging Diesel Spray Nozzles

J. Gao, R. D. Reitz* and J. B. Ghandhi

Engine Research Center, Department of Mechanical Engineering
University of Wisconsin-Madison
Madison, WI 53706 USA

J. Wang and Z. P. Liu

Advance Photon Source, Argonne National Laboratory
Argonne, IL 60439 USA

Abstract

The use of impinging-spray nozzles has been suggested to lower emissions and increase combustion efficiency in direct injection (DI) diesel engines. It has been reported that an impinging-spray nozzle with a relatively small impinging angle (<20 deg.) is favorable in conventional DI diesel engines, especially at high loads, while a nozzle with a larger impinging angle (30-90 deg.) is proposed for early-injected HCCI engines to provide a more homogeneous mixture with shorter penetration and avoid wall contact. The current work is an effort to understand the primary breakup process and macroscale characteristics of diesel sprays with small impinging angle. Two groups of experiments were designed: 1) the near-field of diesel sprays from an impinging-spray nozzle was visualized via an ultrafast X-ray phase-contrast imaging technique. The interior structure and dynamics were elucidated, as compared to the single-hole nozzle spray; 2) to clarify the macroscale characteristics, including the tip penetration and cone angle, equivalent impinging gas jets with various angles were investigated using high-speed schlieren imaging due to the similarity between diesel sprays and gaseous turbulent jets. The results show that an earlier breakup and a complex morphology arises in the impinging spray under steady flow conditions in contrast to the column-like and fairly unperturbed morphology of the single-hole nozzle spray. This is due to instabilities created within the nozzle (presumably geometry-induced turbulence or cavitation). This indicates that the impinging spray nozzle is capable of enhancing fuel atomization, especially in the near-nozzle region. Moreover, it was found that the two jets from an impinging-spray nozzle are already fully atomized before they intersect, and the breakup length is only one or two hole diameters. From the equivalent gas jet experiments it was found that the tip penetration of impinging jets is quite similar to the corresponding single jet. The penetration of the impinging gas jets with small angle (<15 deg. in this study) was found to follow the theoretical correlation established for turbulent single round jets.

Introduction

Recently, the impinging-spray or group-hole nozzle has gained attention in the diesel community. In contrast to the conventional multi-hole nozzle with uniform azimuthal spacing, the nozzle features several groups of orifices, and each group consists of two orifices very close to each other with a converging included angle between them.

Previous studies suggest that nozzles with more and smaller orifices contribute significantly to improved performance and the curtailment of exhaust emissions for direct injection (DI) diesel engines at light- and medium-loads, due to better evaporation and fuel/air mixing (smaller-sized droplets in the fuel spray) [e.g., 1-3]. However, reduced spray tip penetration can be a drawback of decreased orifice diameters, resulting in poor spatial distribution of fuel and air utilization in the combustion chamber, and consequently higher equivalence ratios or concentration gradients locally [4, 5]. This is particularly true for high-speed, high-load conditions, where the in-cylinder gas density is high. It has also been reported that a smaller orifice diameter tends to increase exhaust soot if the lower penetration is not compensated for by higher injection pressure and optimized injection timing [1, 6-8]. To overcome this problem, one promising approach is to use an impinging-spray nozzle with a relatively small impinging angle (usually 0-20 deg., also called the convergent-type group-hole nozzle or cluster nozzle in the literature), instead of the conventional multi micro-hole nozzle. It is expected that the spray from an impinging-spray nozzle has a longer penetration distance, because it has two sources of momentum located close together. Engine experiments have demonstrated the benefits of impinging-spray nozzles in previous studies, especially at high loads [9-11].

*Corresponding author, reitz@engr.wisc.edu

Impinging-spray nozzles with larger impinging angle (typically 30-90 deg.) have been reported to work well in DI diesel homogeneous charge compression ignition (HCCI) engines [12-14]. In studies of spray characteristics, it was found that increasing the impingement angle drastically reduced spray tip penetration, increased the spray angle/volume, and formed a more uniform mixture [12, 15]. These are preferable for combustion in the early-injected-type HCCI engine, where the in-cylinder gas density and temperature are low at the advanced injection timing, thus providing a more homogeneous mixture with shorter penetration and avoiding wall contact.

The current work is an effort to understand the primary breakup process and macroscale characteristics of impinging diesel sprays with small angles. Two groups of experiments were designed: first, the near-field diesel spray from an impinging-spray diesel nozzle with an angle of 5 deg. was observed via an ultrafast X-ray phase-contrast imaging technique, and the interior structure and dynamics were elucidated, as compared to the single-hole nozzle spray. In addition, the macroscale characteristics, including the tip penetration and cone angle, of equivalent impinging gas jets with various angles were investigated using a schlieren technique by exploring the similarities between diesel sprays and gaseous turbulent jets.

Optical Diagnostics, Experimental Apparatus and Procedures

Ultrafast X-ray phase-contrast imaging

The liquid jet atomization consists of two distinctive subprocesses: primary and second breakup. The primary breakup process refers to droplet formation through stripping from the liquid surface, which controls the initial droplet size distribution and velocity [16, 17]. In DI diesel engines, it has a predominant impact on the fuel evaporation, mixture formation, and the whole combustion process. It is well recognized that the high-speed diesel jet breakup starts at the nozzle exit [18]. However, its physics is still not well understood, due not only to its complexity and transient nature, but also to the very high optical density in the near-nozzle field (thus, inaccessible to conventional laser-based diagnostics). Recently, with synchrotron X-ray sources, X-ray radiography and phase-contrast imaging have been used to study the high-speed diesel spray, and have shown the ability to elucidate the interior structure and dynamics of the spray, especially in the near-nozzle field [19, 20]. In this study, the primary breakup process of the impinging spray is studied by the ultrafast X-ray phase-contrast imaging technique.

The X-ray imaging experiment was carried out at the XOR 32-ID beamline of the Advanced Photon Source (APS) at Argonne National Laboratory. The X-ray beam was generated from the APS electron storage ring with a hybrid-singlet fill pattern, in which a single electron pulse (150 ps long) was separated from a train of electrons (472 ns long) by a 1.59 μ s gap on both sides. The X-ray beams passed through a millisecond shutter, a microsecond shutter, and the spray. The transmitted and diffracted X-rays were converted into visible light (434nm) by a fast-scintillator crystal, and were captured with a fast gated CCD camera. A common-rail injection system and specially fabricated solenoid-actuated injectors with single (group) orifices were used to inject diesel fuel into a quiescent nitrogen gas ambient. The spray chamber features a gentle flow of the nitrogen gas (at atmospheric pressure and room temperature) to scavenge the fuel vapors. The shutters, CCD camera, and injection system were synchronized to the X-ray pulses using Stanford DG535 delay generators. More detailed discussion on the experimental apparatus can be found in [19, 20]. The injection energizing time was set to 1 ms for all test cases. The exposure time was 1.5 μ s for the spray imaging. The field of view of the imaging system was 1.36 X 1.71 mm² with a spatial resolution of 1.34 μ m/pixel.

High-speed schlieren imaging

There exist great similarities between diesel sprays and gaseous turbulent jets when a scaling factor is used which is defined as the equivalent diameter d_{eq} [21, 22]. Thus, the macroscale characteristics of impinging gas jets were also investigated to aid the understanding of impinging diesel sprays with a schlieren technique.

A double-pass schlieren system was used [23]. Since the light passes through the test section twice and is, therefore, deflected by the density gradients twice, the sensitivity of this type of system is naturally greater than that of a Z-type system. The experimental setup is similar to that described in [24]. Two outwardly opening poppet-type gaseous injectors were installed face-to-face in a machined housing. The space between the two injector poppets formed the sac volume, which was minimized to provide short response times. Removable orifice-containing plates were attached to the top of the assembly and communicated with the sac through a short passage. The sac pressure was measured using a Kulite XT-190 absolute pressure transducer and an oscilloscope. Helium was selected as the injection medium, and was supplied to the injector at different pressures. The helium jet was injected into the ambient atmosphere at room temperature. The injection timing and image acquisition were controlled by a Berkeley Nucleonics model 555 delay generator. For each experiment, the energizing time was set to 10 ms, and the injection profile was a "Flat" shape (steady injection). The ratio of the injection pressure to the ambient pressure was kept below 2 so that the Mach number at the nozzle exit is less than 1. The actual gas flow rate at different pressure ratios was measured by a bellows gas meter under steady flow conditions prior to the experiments. The images were re-

corded at a speed of 10,000 fps. The image resolution was 512 X 248 pixels with a spatial resolution of 0.19 mm/pixel.

Image processing

For the acquired X-ray and schlieren images, each image was 3 X 3 median filtered, and then an enhancement algorithm was applied, viz., $\text{new image} = [(\text{raw image}/\text{background image}) - 1] \cdot S + 128$. Background images recorded prior to injection were also median filtered, and the constant S was set to 300. The enhancement algorithm evened out background intensity, increased contrast, and eliminated imperfections in the optics. The image processing was carried out using Matlab software. To evaluate the jet tip penetration and cone angle in the schlieren images, a procedure similar to that of Naber and Siebers [21] was adopted. An intensity threshold level was used to separate the jet region from the background ambient gas. The final threshold level was chosen to allow automated processing of the images without affecting accuracy. Then, the jet penetration and cone angle were evaluated through an iterative process, since the definition used for each depends on the other. The penetration was defined as the distance along the jet axis to a location where 1/2 of the pixels on an arc of $\theta/2$ centered on the jet axis were within the jet. The jet cone angle (θ) was measured based on the projected area between the 10% and 80% location of the jet penetration.

Results and Discussion

Primary breakup process of impinging diesel sprays

Two specially fabricated diesel nozzles were used. The impinging-spray nozzle had two 0.096mm diameter micro holes with a 5 deg. converging included angle between them. The inter-hole spacing between the two holes was 0.3 mm. The other nozzle had an axial single-hole with a diameter of 0.135mm (equivalent hole area to that of the impinging-spray nozzle). The hole length for both nozzles was 0.8 mm. These specifications are comparable to those of nozzles used in practical diesel injectors. X-ray images of the nozzles (**Fig.1** insets) indicate that these specially fabricated nozzles have undergone very little hydrogrinding, leaving a sharp entrance to the nozzles.

Figure 1 shows X-ray phase-contrast images of the diesel spray from the two nozzles at 900bar injection pressures. Image frames taken at different distances from the nozzle exit were stitched together to give an overall view of the primary breakup process (frames were not taken concurrently). In sharp contrast to conventional laser-based imaging measurements (e.g., [25]), the internal features of the spray are clearly visualized in the X-ray phase-contrast images with ultrahigh temporal and spatial resolution. The image contrast comes from boundaries and interfaces between materials with different refraction index or abrupt thickness variations [20]. In all cases, the jets possess a very smooth morphology in the very near nozzle region, suggesting that they remain as a liquid column rather than breaking into droplets. Unsteady waves are then observed on the liquid surface, indicating the onset of atomization. The distance between the nozzle exit and the location where surface disturbances are obvious (the length of the intact liquid column), which is referred to as the breakup length, varies from a few nozzle diameters to several millimeters. It appears to be dependent on the nozzle structure and flow condition (acceleration vs. quasi-steady state), whereas the injection pressure/velocity only has a minor impact. Further downstream, the jet exhibits a complex internal structure because of turbulence in the flow, and therefore is considered to be full atomized.

Qualitative differences between the two nozzles are easily recognizable. During the acceleration flow state ($45\mu\text{s}$ in **Fig.1**), the jets from both nozzles have a relatively short breakup length at the two injection pressures, approximately only two or three hole diameters. However, under quasi-steady flow conditions ($510\mu\text{s}$ in **Fig.1**), the unsteady surface waves arise much more quickly and chaotically in the case of the impinging-spray nozzle. The spray from the single-hole nozzle seems to have a much longer liquid core which extends far downstream of the nozzle exit (several millimeters), since it has a column-like and fairly unperturbed morphology in this region. These observations imply that different mechanisms contribute to the jet breakup under various conditions. The current view based on experimental and modeling evidence is that cavitation, turbulence-driven instability, and aerodynamics shear are widely recognized mechanisms for the primary breakup process [17, 18]. The present images confirm that the earlier jet breakup of the impinging-spray nozzle at the steady flow state is due to instabilities created within the nozzle. It is believed that flow interferences between the holes at their inlets (or the larger specific surface area) cause stronger geometry-induced turbulence or cavitation within the holes. In contrast, the flow into the nozzle hole of the single-hole nozzle is less disturbed and the fuel can better stream into the nozzle. As a result, a much longer liquid core remains. Second, the higher initial disturbance level introduced by the unsteady flow may play a role in the jet breakup during the acceleration phase. In addition, aerodynamic shear appears to be less important in the primary breakup, but may be responsible for secondary breakup [17]. To understand the breakup process of impinging sprays more closely, the snapshots were taken and compared during the initial stages of the injection, as shown in **Fig.2**. As mentioned above, it is observed that the two jets breakup very quickly after exiting the nozzle and the breakup length is only two or three hole diameters. The two jets intersect at a location about 1 mm downstream from the nozzle exit, and thereafter, the jets merge into each other completely, and behave as a single spray.

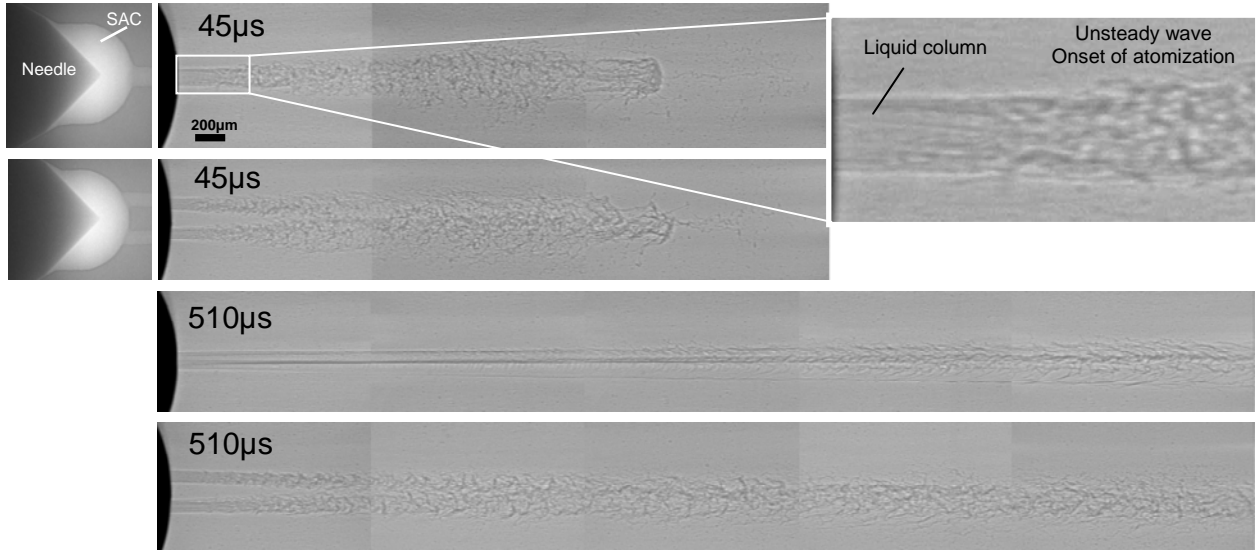


Fig. 1 X-ray phase-contrast images of diesel sprays from impinging-spray and single-hole nozzles ($p_{inj}=900\text{bar}$)

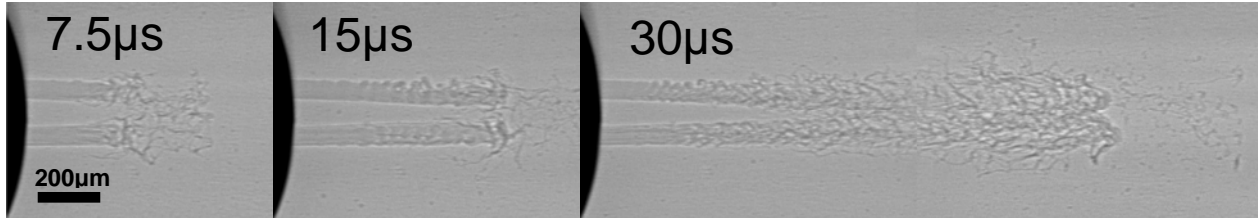


Fig.2 Snapshots of the diesel spray from the impinging-spray nozzle during the initial stages of injection

The above results provide direct confirmation of some important features in impinging diesel sprays. First, the images explain why the impinging angle [12] and impinging distance [26] have a fairly small impact on the measured droplet diameters (overall Sauter mean diameter, SMD). This is because the two jets from the impinging-spray nozzle are already atomized before they intersect, regardless of the very close spacing. Jet merging (sheet formation) and collision-induced turbulence are not the controlling factors for breakup. In addition, as recently revealed by CFD calculations [27], the SMDs of group-hole nozzle sprays are much lower than those of the single-hole nozzle with same hole area in the near-field of the spray. The observations on the primary breakup processes in this study strongly support this conclusion.

Macroscale characteristics of impinging gas jets

Four converging double-hole nozzles were used in gas jet experiments to simulate the above impinging-spray nozzles. The diameter of each hole and the hole length of all test nozzles were 0.5 mm and 4 mm, respectively. The included-angle between the two holes was varied from 0 to 15 deg. in steps of 5 deg. The inter-hole spacing at the nozzle exit was 1.5 mm for all nozzles. Hereafter, they are termed the DH0.5/0, DH0.5/5, DH0.5/10 and DH0.5/15 nozzle, respectively. Two single-hole nozzles were also tested for comparison: SH/0.7 nozzle with hole diameter of 0.7mm (with the same total hole area as that of the double-hole nozzle); and SH/0.5 nozzle, which had the same hole diameter as that of the double-hole nozzle. These parameters were determined through scaling the corresponding diesel nozzle by the factor $d_{eq} = d_{noz} \cdot (\rho_l/\rho_g)^{1/2}$, where d_{noz} is the nozzle diameter, ρ_l and ρ_g are the liquid and gas-phase densities [28].

Figures 3a, b and c show jet images, measured jet tip penetrations and cone angles for all test nozzles at 500m/s exit velocity. For all cases, the jet tip penetration is found to increase with increasing exit velocity, while the cone angle stabilizes to a value around 30 deg. after about 3ms start of injection. The high value of the initial cone angle is due to relatively poor resolution near the nozzle exit. In the front view images, the two individual jets issuing from the double-hole nozzles can be readily seen in the very near-nozzle field. However, they quickly collide and merge, and cannot be distinguished downstream. The impingement details of the jets clearly have a fundamental impact on

the macroscale characteristics of the jet. The jets from the double-hole nozzles present an increased tip penetration and a wider front view cone angle than that of the SH0.5 nozzle. From the side view, the cone angles vary very little amongst all tested nozzles. The impinging angle appears to have small effects on the macroscale characteristics of the jet, and the jet shapes of the double-hole nozzles are very similar to that of the SH0.7 nozzle, except for a slight decrease in the tip penetration. The DH0.5/5 nozzle has the farthest penetration distance amongst the double-hole nozzles at the three exit velocities, whereas the DH0.5/15 has lower jet tip penetration presumably due to the greater momentum loss.

Based on the self-similar configuration of the free turbulent gas jet from a single round hole, theoretical correlations on the jet-tip penetration have been developed based on momentum conservation [28, 29, 22]. The parameters that most influence the jet penetration are ambient density ρ_a and momentum flow rate \dot{M} supplied by the orifice. For the steady turbulent jet, all correlations show the same dependence of these parameters,

$$S = \Gamma \cdot (\dot{M} / \rho_a)^{1/4} \cdot t^{1/2} \quad (1)$$

in which S is the jet tip penetration, t is the time from start of injection, and Γ is the scaling constant. To examine the validity of equation (1) for impinging gas jets, all of the data of **Fig.3b** were recast, as shown in **Fig.3d**. For the double-hole nozzles, the momentum flow rate was evaluated as $\sqrt{2} \cdot \rho_n \cdot (\pi/4) \cdot d_n^2 \cdot U_n^2$, in which ρ_n is the injected gas density calculated from compressible flow equations, d_n is the hole diameter, and U_n is the exit velocity. It is clear that gas jets with a small impingement angle also exhibit self-similar behavior. Note that the scaling constant Γ is found to be approximately 3.0 in this study, which agrees very well with the recommended value (3.0 ± 0.1) in [28, 29]. Thus, it is concluded that the tip penetration of impinging gas jets is predictable using correlation (1).

Implications for DI diesel engines

From the above results, it is seen that the impinging-spray nozzle enhances fuel atomization, especially in the near-nozzle field, as compared to the conventional nozzle. Therefore, this type nozzle with small angle (e.g., 5 deg.) may have potential to improve engine performance by forming a more uniform fuel/air mixture without sacrificing spray tip penetration. However, further investigation is required at high ambient density conditions. Considering the fact that the two jets from the impinging-spray nozzle are already atomized before they intersect, the mixture spatial distribution in the combustion chamber might be controllable through the impinging angle and distance to fit the demands of different combustion modes (like HCCI) without adversely affecting the atomization quality.

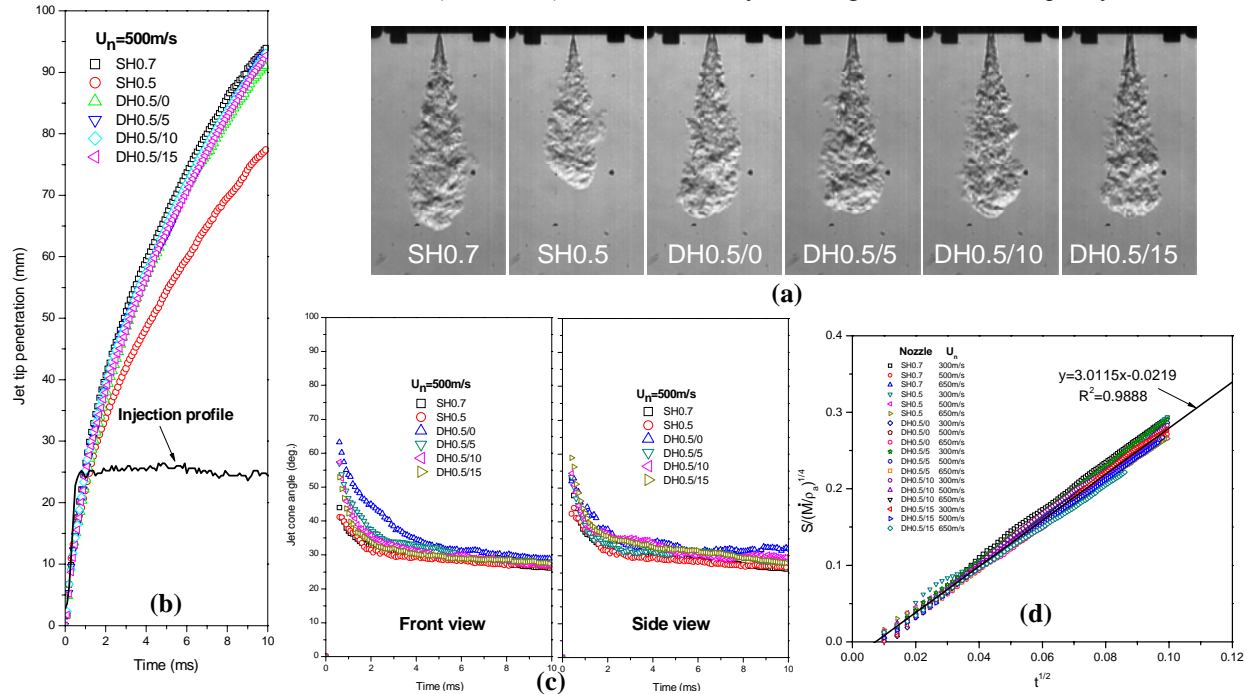


Fig.3 Macroscale characteristics of equivalent gas jets from the single- and double-hole nozzles. (a) Schlieren gas jet images taken at 5ms after the start of injection (front view, helium into air, 500m/s exit velocity); (b), (c) jet tip penetration and cone angle at 500m/s exit velocity; (d) nondimensional gas jet penetration for all of the data

Conclusions

The behavior of impinging diesel sprays and equivalent gas jets has been investigated experimentally. The diagnostics include use of ultrafast X-ray phase-contrast imaging and high-speed schlieren imaging to visualize the primary breakup process of diesel sprays in the very near-nozzle field and gas jet injection, respectively.

The X-ray images show for the first time that, due to instabilities created within the nozzle (presumably geometry-induced turbulence or cavitation), unsteady waves arise on the liquid surface much more quickly and chaotically in the case of the impinging-spray nozzle as compared to the corresponding single-hole nozzle, indicating earlier jet breakup. The impinging spray also has a more complex near-nozzle morphology at the steady flow state. Therefore, the impinging spray nozzle enhances the fuel atomization, especially in the near-nozzle field. It was observed that the two jets from the impinging-spray nozzle are already atomized before they intersect regardless of their very close spacing. This explains why the impinging angle and distance have a fairly small impact on measured droplets diameters (overall SMD).

From the equivalent gas jet experiments and the diesel sprays, it is concluded that the tip penetration of impinging jets is quite similar to that of the corresponding single jet. Moreover, the penetration of impinging gas jets with small impingement angles ($<15^\circ$) was found to be predictable using correlations for turbulent single round jets, based on self-similarity and momentum conservation. Finally, it is suggested that an impinging-spray nozzle with small angle (e.g., 5° in this study) has potential to improve engine performance by forming a more uniform fuel/air mixture without sacrificing spray tip penetration.

Acknowledgments

Use of the Advanced Photon Source was supported by the U.S. Department of Energy, Office of Science, Office of Basic Energy Sciences, under Contract No. W-31-109-Eng-38. The authors would like to thank Denso Corp. and Nippon Soken Inc., Japan, for providing the injectors. Especially, Mr. Takaaki Sato, Nippon Soken Inc., is highly appreciated for his technical support and discussion. The authors also appreciate technical support from Dr. Kamel Fezzaa, X-ray Science Division, Argonne National Laboratory, and Dr. Xingbin Xie, Wayne State Univ., in conducting the experiments, and helpful discussions with Neerav Abani, Univ. of Wisconsin-Madison.

References

1. Montgomery, D. T., Chan, M., Chang, C. T., Farrell, P. V. and Reitz, R. D., SAE paper 962002 (1996).
2. Kobori, S., Kamimoto, T. and Kosaka, H., SAE paper 960321 (1996).
3. Hotta, Y., Nakakita, K., Fuyuto, T., Inayoshi, M., Fujiwara, K. and Sakata, I., SAE paper 2002-01-1160 (2002).
4. Su, T. F. and Farrell, P. V., *Atomization and Sprays*, 8(1): 83–107 (1998).
5. Arregle, J., Pastor, J. V. and Ruiz, Z., SAE paper 1999-01-0200 (1999).
6. Benajes, J. *et al.*, *Proceedings of I MECH E Part D: Journal of Automobile Engineering*, 220: 1807-1817 (2006).
7. Hotta, Y., Nakakita, K., Fuyuto, T., Inayoshi, M., Fujiwara, K. and Sakata, I., SAE paper 2002-01-1160 (2002).
8. Matsumoto, A., Xie, X., Lai, M.-C., Winsor, R. E. and Huynh, T. C., SAE paper 2008-01-2424 (2008).
9. Tokuda, H. *et al.*, *Proceedings of the 26th Vienna Motor Symposium*, Vienna, Austria (2006).
10. Adomeit, P., *et al.*, *THIESEL Conference*, Valencia, Spain (2006).
11. Dohle, U., *et al.*, *Proceedings of the 26th Vienna Motor Symposium*, Vienna, Austria (2006).
12. Iwabuchi, Y., Kawai, K., Shoji, T. and Takeda, Y., SAE paper 1999-01-0185 (1999).
13. Nordgren, H., Hultqvist, A. and Johansson, B., SAE paper 2004-01-2990 (2004).
14. Wahlin, F., Cronhjort, A., Olsson, U. and Angstrom H. E., SAE paper 2004-01-2989 (2004).
15. Wahlin, F. and Cronhjort, A., SAE paper 2004-01-1776 (2004).
16. Lin, S. P. and Reitz, R. D., *Annu. Rev. Fluid Mech.*, 30: 85-105 (1998).
17. Smallerwood, G. and Gulder, O. L., *Atomization and Sprays*, 10: 355–386 (2000).
18. Reitz, R. D. and Bracco, F. V., *Phys. Fluids*, 25: 1730-1742 (1986).
19. Wang, J. *Journal of Synchrotron Radiation*, 12: 197-207 (2005).
20. Wang, Y. *et al.*, *Nature Physics*, 4:305-309 (2008).
21. Naber, J. D. and Siebers, D. L., SAE paper 960034 (1996).
22. Desantes, J. M., Arregle, J., Lopez, J. J. and Cronhjort, A., *Atomization and Sprays*, 16: 443–473 (2006).
23. Petersen, B. R. and Ghandhi, J. B., SAE paper 2006-01-0652 (2006).
24. Abani, N., Ghandhi, J. B. and Reitz, R. D., *THIESEL Conference*, Valencia, Spain, (2008).
25. Gao, J., Matsumoto, Y. and Nishida, K., *Atomization and Sprays*, 19(4): 321–337 (2009).
26. Chiba, T., Saito, M., Amagai, K. and Arai, M., *Atomization and Sprays*, 12: 431–449 (2002).
27. Park, S. W. and Reitz, R. D., submitted to *Atomization and Sprays*.
28. Abraham, J., *Numerical Heat Transfer, Part A*, 30: 347-363 (1996).
29. Hill, P. G. and Ouellette, P., *Journal of Fluids Engineering*, 121: 93-101 (1999).